

Chapter 4

Development of *B. subtilis* DK1042

secreting oxalic acid

and

characterization of mineral phosphate

& potassium solubilization ability

4.1 Introduction

Plant growth promoting rhizobacteria (PGPR) are known to promote plant growth through variety of mechanisms such as nutrients mobilization, production of plant growth hormones, inducing abiotic stress tolerance, and biocontrol of plant pathogens. However, efficacy of plant growth promotion depends on the abundance and functional status in the rhizosphere. Mineral solubilization ability of rhizobacteria is mainly due to secretion of organic acids such as gluconic acid, 2-keto gluconic acid, citric acid, malic acid, oxalic acid, etc. (Goldstein, 1996; Gyaneshwar et al., 1999; Sharma et al., 2005; Alori et al., 2017). Srivastava et al. (2006) reported the phosphate solubilization efficacy of different organic acids in alfisol solution amended with rock phosphate 40 mg/g of soil and it was found that oxalic acid and citric acid were the most effective (Table 4.1).

Table 4.1: Efficacy of different organic acids at P-solubilization from alfisol supplemented with RP (40 mg/g soil).

Organic acid	Concentration (mM)	0 h		24 h	
		pH	Solution P (µM)	pH	Solution P (µM)
None	-	6.73±0.21	U.D.	6.69±0.02	U.D.
Oxalic	10	3.42±0.05	1560±4.0	3.14±0.01	1092±2.4
Citric	10	3.45±0.04	409±8.0	3.22±0.02	387±3.0
Citric	20	2.80±0.034	850±6.5	3.18±0.431	646±2.9
Tartaric	20	3.50±0.02	550±6.0	3.60±0.23	502±2.1
Gluconic	50	3.40±0.05	800±2.0	3.71±0.01	300±5.0
Lactic	50	3.25±0.015	920±7.0	3.36±0.02	200±3.0
Succinic	50	3.64±0.04	332±7.0	3.66±0.07	359±5.3
Acetic	50	3.80±0.23	102±2.0	4.45±0.3	80±2.0

While studying the effect of oxalic and citric acid on dynamics of potassium (K) release from feldspar and mica, Song and Huang (1988) found that the order of K release from K bearing minerals is biotite > microcline orthoclase > muscovite. Oxalic acid is naturally produced in high quantities by variety of fungi (Kubicek, 1987; Gadd, 1999). Oxalate secretion by fungi serves important functions such as colonization of substrates (Dutton and Evans, 1996), increased bioavailability of nutrients (Schmalenberger et al., 2015), reduction in metal toxicity (Fomina et al., 2005), competitive advantage by lowering the pH of surroundings (Andersen et al., 2009; Poulsen et al., 2012) and virulence factor (Kirkland et al., 2005) etc.

Aspergillus niger is recognized as the best producer of oxalic acid (Strasser et al., 1994; Podgórski and Leśniak, 2003; Musial et al., 2006). Very high intra and extra cellular concentration of oxalate is detrimental to the organism producing it and therefore, these organisms possess different mechanisms for preventing such damage. Some of these organisms have oxalate degrading capacity and they convert oxalate into CO₂ (Espejo and Agosin, 1991; Micales, 1995; Schilling and Jellison, 2005) while others utilize various transporters for secretion of oxalic acid and thereby reducing the intracellular oxalic acid (Malony, 1994; Cheng et al., 2007; Watanabe et al., 2010). Secretion of oxalate in *Formitopsis palustris* is achieved by efflux transporter FpOAR (*Fp* oxalic acid resistance). Secretion of organic acids results in nutrient mobilization mainly by two mechanisms: proton mediated and ligand mediated. Ionization of organic acid molecules results in the increased H⁺ concentration which accelerates the solubilization by attaching to the oxygen in –OH groups bridging the metals, thus removing electron density and weakening the bond of metal-oxygen linkage. Ligand-cation interaction at the mineral surface is thought to polarize and weaken the bond between the cation and mineral lattice (Manley and Evans, 1986; Burgstaller and Shinner, 1993; Muller et al., 1995; Ullmann and Welch, 2002; Burford et al., 2003).

Very few bacterial strains such as *Chitinophaga jiangningensis* JN53, *P. fluorescence* ATCC 13525 and *Burkholderia* (Hamel et al., 1999; Nakata & He, 2010; Nakata, 2011; Cheng et al., 2017) are known to produce oxalic acid. *P. fluorescens* ATCC 13525 produced oxalic acid as a glyoxylate intermediate in a mineral medium containing citric acid as sole carbon source in response to aluminum stress. Two genes,

obcA and *obcB*, organized in an operon are responsible for oxalic acid biosynthesis in *Burkholderia mallei* and *Burkholderia glumae* where oxalic acid was reported to serve as pathogenicity factor. *C. jiangningensis* JN53 produced 0.8 mg L⁻¹ and oxalic acid in Bushnell-Haas medium (BHm) containing biotite and it produced 98 mg L⁻¹ in modified BHm medium containing potassium feldspar.

The precursor for oxalic acid is oxaloacetate, which occurs at the anaplerotic node connecting glycolysis, gluconeogenesis and tricarboxylic acid (TCA) cycle. Oxaloacetate is synthesized by two mechanisms: one is via the action of pyruvate carboxylase (PycA) (Sauer and Eikmanns, 2005) encoded by *pycA* and the other is by malate dehydrogenase (Mdh) encoded by *mdh* (Meyer and Stulke, 2012). Metabolic flux analysis using glucose as the sole carbon source in seven (aerobic batch culture) different bacteria revealed that relative TCA cycle flux was much lower in *B. subtilis* and *E. coli* than that in the other species because of secretion of the incompletely oxidized overflow product acetate was extensive. In order to increase the amount of oxaloacetate, it is necessary to reduce the incomplete oxidation of the carbon source and to increase the flux in TCA cycle.

Vitreoscilla hemoglobin has been expressed in variety of host organisms to increase the oxygen availability so as to enhance the growth and subsequently the production of myriad of metabolites (Magnolo et al., 1991; Holmberg et al., 1997; Frey and Kallio, 2003; Li et al., 2005; Wang et al., 2009; Wu et al., 2015). VHB was the first bacterial hemoglobin discovered from a Gram-negative bacterium *Vitreoscilla* sp. CI (Webster and Hackett, 1966). It is a homodimeric protein which acts as an excellent oxygen carrier and transporter due to its very high dissociation constant for oxygen (Webster and Hackett, 1966; Orri and Webster, 1986). Expression of VHB in *E. coli* and *B. subtilis* resulted in the reduction of metabolic flux through energetically inefficient fermentative pathways (Kallio and Bailey, 1996; Roos et al., 2004). *Bacillus* has been one of the dominant plant growth promoting rhizobacteria (PGPR) with efficient biocontrol properties involving secretion of antimicrobial compounds and enzymes. Since the *Bacillus* spp. possesses good biocontrol abilities and mycorrhizal helper ability, *Bacillus* spp. with phosphate and potassium solubilizing properties could be a very effective PGPR.

4.2 Rationale

Present study aims to determine the effect of incorporation of *vgb* gene along with artificial oxalate operon, containing oxaloacetate acetyl hydrolase (*oah*) and oxalic acid transporter (*FpOAR*) genes, on oxalic acid production, secretion, mineral phosphate and potassium solubilizing ability in *B. subtilis* DK1042.

4.3 Work plan

4.3.1 Bacterial strains used in this study

Table 4.2 Bacterial strains used and constructed in this study

Bacterial Strains	Genotype	Reference
<i>E. coli</i> DH10B	<i>F</i> ^{endA1} <i>recA1</i> <i>galE15</i> <i>galk16</i> <i>nupGrpsL</i> Δ <i>lacX74</i> Φ 80 <i>lacZ</i> Δ <i>M15</i> <i>araD139</i> Δ (<i>ara</i> , <i>leu</i>) 7697 <i>mcrA</i> Δ (<i>mrr</i> - <i>hsdRMS</i> - <i>mcrBC</i>) ^{λ-}	Invitrogen
DH10B (pNRM2)	<i>E. coli</i> DH10B with plasmid pNRM2; Amp ^r	This study
DH10B (pNRM4)	<i>E. coli</i> DH10B with plasmid pNRM4; Amp ^r	This study
DH10B (pNRM5)	<i>E. coli</i> DH10B with plasmid pNRM5; Amp ^r	This study
DH10B (pNRM6)	<i>E. coli</i> DH10B with plasmid pNRM6; Amp ^r	This study
DH10B (pNRM157)	<i>E. coli</i> DH10B with plasmid pNRM157; Amp ^r ; Km ^r ; Neo ^r	This study
DH10B (pNRM1113)	<i>E. coli</i> DH10B with plasmid pNRM1113; Amp ^r ; Km ^r ; Neo ^r	This study
DH10B (pNRM1114)	<i>E. coli</i> DH10B with plasmid pNRM1114; Amp ^r ; Km ^r ; Neo ^r	This study
DH10B (pNRM110)	<i>E. coli</i> DH10B with plasmid pNRM110; Amp ^r ; Km ^r ; Neo ^r	This study
<i>B. subtilis</i> DK1042	NCIB 3610 <i>ComI</i> ^{Q12L}	BGSC, Konkol et al., 2013

NRM1113	<i>B. subtilis</i> DK1042 <i>amyE::P43-lox71-Kan-lox66-P43-vgb-gfp</i>	This study
NRM1114	<i>B. subtilis</i> DK1042 <i>amyE::P43-lox71-Kan-lox66-(P43)₄-vgb-gfp</i>	This study
NRM110	<i>B. subtilis</i> DK1042 <i>amyE::P43-lox71-Kan-lox66-(P43)₄-vgb-gfp-P43-FpOAR-oah</i>	This study

4.3.2 Cloning of promoterless *oah* in pUC18

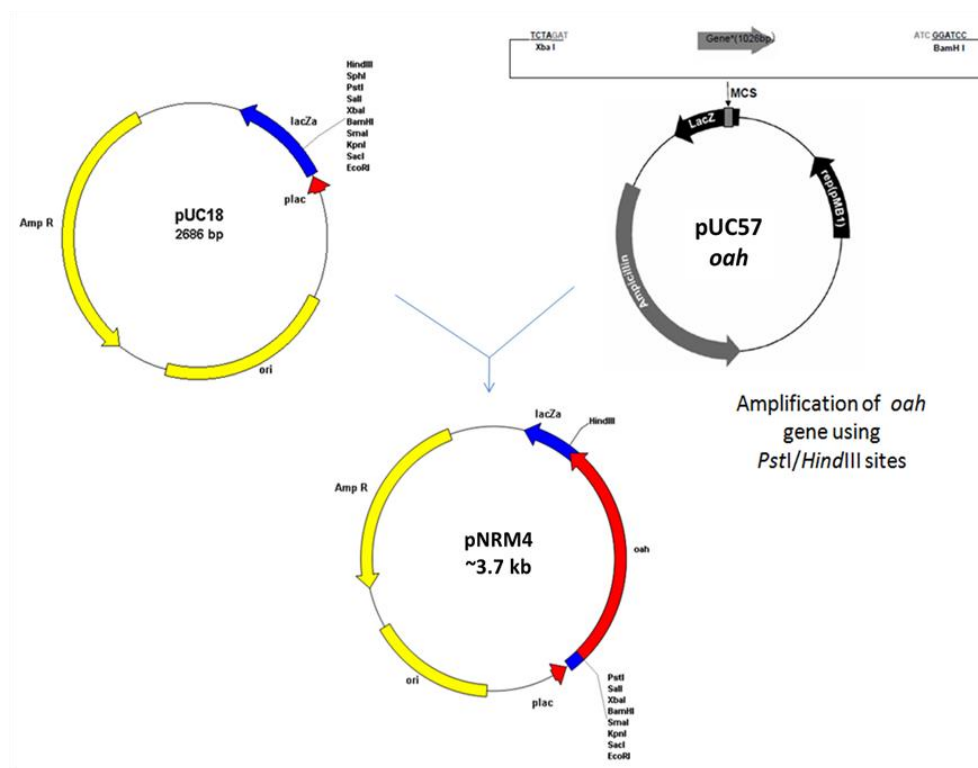


Fig. 4.1: Schematic representation of cloning of *oah*

4.3.3 Construction of plasmid pNRM5 containing P43-*FpOAR-oah* operon

B. subtilis codon optimized *oah* gene was amplified from pUC57*oah* plasmid using *oahF* and *oahR* primers followed by digestion with PstI and HindIII and ligation in to pUC18. Primer sequences used for cloning of *oah* gene are as follow; restriction sites are italicized and ribosome binding site (RBS) is underlined.

oahF - 5' – TGC ACT GCA GAT ATT AAG AGG AGG AGA ATA CAA ATG
AAG GTG GAC ACC CCG GAT A – 3'

*oah*R - 5' – CC AAG CTT TCA CAC GCC GTT GGC GAA A – 3'

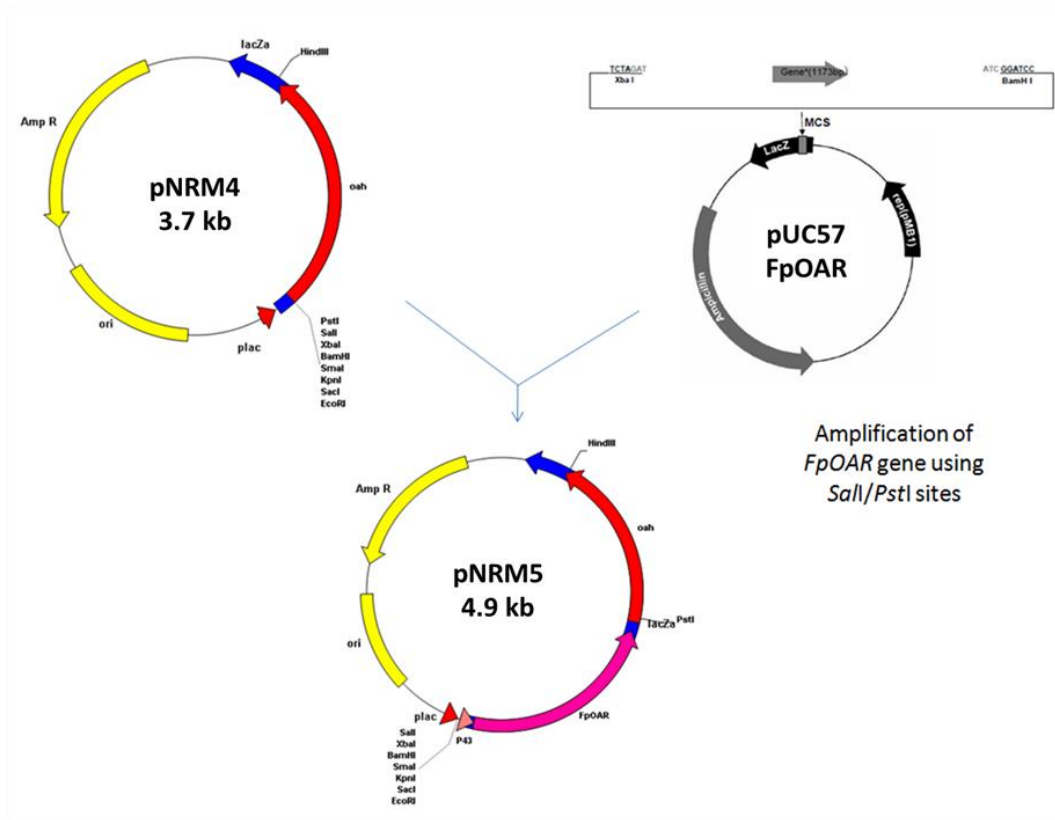


Fig. 4.2: Cloning of P43-FpOAR upstream of *oah* in pNRM4.

As described earlier in section 3.3.3.2, two different forward primers and a reverse primer were designed to clone *B. subtilis* codon optimized *FpOAR* and to incorporate *P43* promoter. Primer sequences are as follows; restriction sites are italicised and RBS are underlined. *P43* promoter sequence is highlighted in red colour and overlapping region between both the forward primers is highlighted in bold.

FpOARF1 - 5' – GCG TCG ACA TTT TAC ATT TTT AGA AAT GGG CGT GAA
AAA AAG CGC GCG ATT ATG TAA AAT ATA AAT AAT ATT AAG AGG
AGG AGG A ATA – 3'

FpOARF2 - 5' – GCG CGC GAT TAT GTA AAA TAT AAA TA **A TAT TAA**
GAG GAG GAG AAT ACA AAT GAC CGA TCT GCA CCG CAG – 3'

FpOARR- 5' –TGC ACT GCA G TC ACA GCA GGT CCT CTT GAC GC - 3'

B. subtilis codon optimized *FpOAR* was amplified using *FpOARF2* and *FpOARR* from pUC57*FpOAR* plasmid containing *FpOAR* gene. *FpOARF2R* amplicon was purified using PCR clean up kit (Nucleopore Quick PCR Purification Kit, Genetix Biotech Asia Pvt. Ltd.) and this purified amplicon was used as template to incorporate complete sequence of *P43* promoter using *FpOARF1* and *FpOARR* primers. The amplicon obtained after the second PCR was designated as *FpOARF1R*. Thus, *FpOARF1R* amplicon consisted of forward restriction site *SalI* - *P43* promoter – RBS – *FpOAR* and reverse restriction site *PstI*. *vgbF1R* amplicon was digested with *SalI* and *PstI* and was ligated into pNRM4 to give rise to pNRM5. Thus, pNRM5 contains a bicistronic operon containing *FpOAR* and *oah* gene under the control of constitutive *P43* promoter.

4.3.4 Construction of plasmid pNRM6 containing two bicistronic operons *P43-FpOAR-oah* and *P43-vgb-gfp*

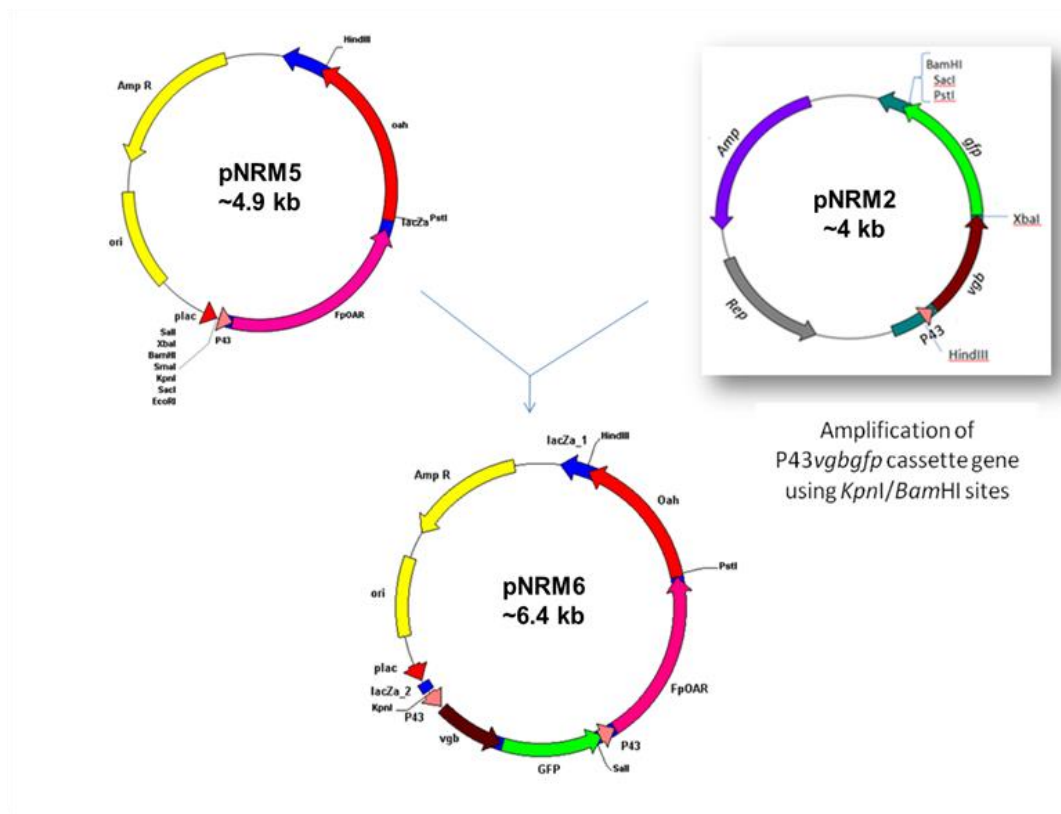


Fig. 4.3: Schematic representation of construction of plasmid pNRM6.

generate one blunt end. Then it was digested with KpnI to create one sticky end. Similarly, pNRM6 was digested with HindIII and the linearized vector was treated with Klenow fragment to generate one blunt end. Then it was digested with KpnI to create one sticky end. Thus, directional cloning of *P43-vgb-gfp* and *P43-FpOAR-oah* operons downstream of *P43* tandem repeats was carried out.

4.3.6 Transformation of *E. coli* and *B. subtilis* DK1042 with respective vectors

4.3.6.1 Development of *E. coli* transformants harboring plasmid pNRM5

As mentioned in section 2.3.7.1, *E. coli* DH10B and *E. coli* BL21DE3 were transformed using MgCl₂-CaCl₂ method (Sambrook and Russell 2001). All the plasmid transformants were screened for ampicillin resistance (Amp^r).

4.3.6.2 Development of *B. subtilis* DK1042 integrants harboring plasmid pNRM110

As mentioned in section 2.3.7.2, *B. subtilis* DK1042 was transformed with the integration vectors pNRM1113 and pNRM1114 using natural competence method and the integrants thus obtained were designated as NRM1113 and NRM1114, respectively. The *Km^r* gene also confers resistance to neomycin antibiotic in *B. subtilis* DK1042 therefore; the integrants were screened for neomycin resistance and neomycin resistant colonies of *B. subtilis* DK1042 were then reconfirmed for integration at *amyE* and not any other place in the genome using starch agar plate.

4.3.7 Oxalic acid production and secretion in *E. coli* BL21DE3 and *B. subtilis* DK1042 harboring artificial oxalate operon

E. coli BL21DE3 is the most preferable expression host to study the expression of heterologous genes and the functionality of the protein products therefore, *E. coli* BL21DE3 containing pNRM5 was grown in Tris-rock phosphate broth (section 2.2.3) containing 100 mM Glucose, 50 mM Tris and 1 mg/ml rock phosphate. Presence of oxalic acid in the culture supernatant was determined qualitatively as well as quantitatively. All samples taken from bacterial culture were centrifuged (10 min at 10000 rpm at room temperature) and 2 ml of the supernatant was filtered through a 0.22 micron membrane filter (Millipore, Bedford, MA, USA) before injection.

Quantitative HPLC was performed on a Shimadzu HPLC, a 210nm wavelength UV–vis detector and Acclaim OA HPLC column was used. The mobile phase was composed of 100 mM Na₂SO₄ (adjusted to pH 2.65 with methane sulfonic acid). It was filtered through a 0.45 mm membrane filter (Millipore) and pumped to the column at a flow rate of 0.6 ml min⁻¹. The run time was set at 15 min and the column temperature was maintained at 25 °C. The volume of injection was 5 µl. Prior to injection of the samples, the column was equilibrated for at least 30 min with the mobile phase flowing through the systems. Detection was carried out at 210 nm. The resolution peaks were recorded on the HPLC chart according to the retention time of each compound.

Similarly, *B. subtilis* DK1042 WT, DK1042 NRM1113, DK1042 NRM1114 and DK1042 NRM1110 were grown in M9 minimal broth (Kleijn et al., 2010). Two different carbon sources used were as follows: M9 broth with 50 mM Glucose (GM9) and M9 broth with combination of 50 mM Glucose + 20 mM Malate (GMM9). Growth and pH of DK1042 WT and integrants were monitored at regular time intervals to analyze acid secretion. Oxalic acid secretion was determined by using HPLC.

4.3.8 Effect of heterologous expression of *P43-FpOAR-oah* operon on Mineral Phosphate Solubilization (MPS) and Mineral Potassium Solubilization (MKS) ability of *B. subtilis* DK1042, NRM1113, NRM1114 and NRM1110

MPS and MKS ability of DK1042 and integrants was determined on Pikovaskaya's agar and Aleksandrov agar (**section 2.2.2**), respectively. Saline washed bacterial inoculum (5 ml) was spot inoculated on plates and incubated at 30 °C. Phosphate and potassium solubilization and acid secretion was determined by monitoring the growth and formation of zone of clearance surrounding the bacterial growth.

4.4 Results and Discussion

4.4.1 Construction of artificial oxalate operon

Cloning of different genes in different vectors was confirmed by restriction digestion pattern analysis post cloning.

4.4.1.1 Construction of pNRM4

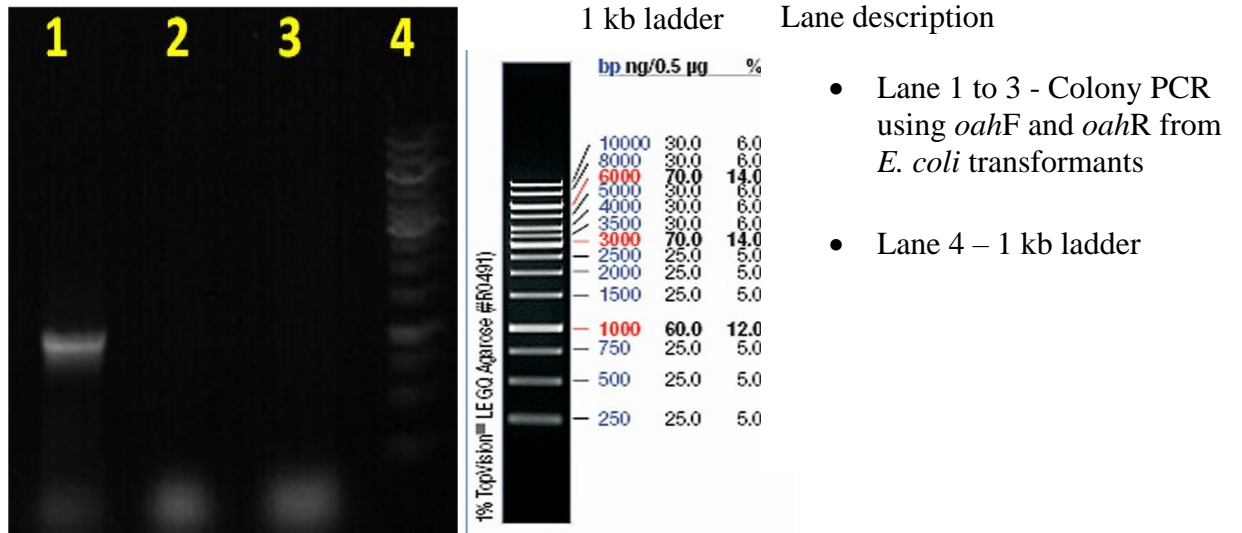


Fig. 4.5: Colony PCR of *oah* from *E. coli* transformants.

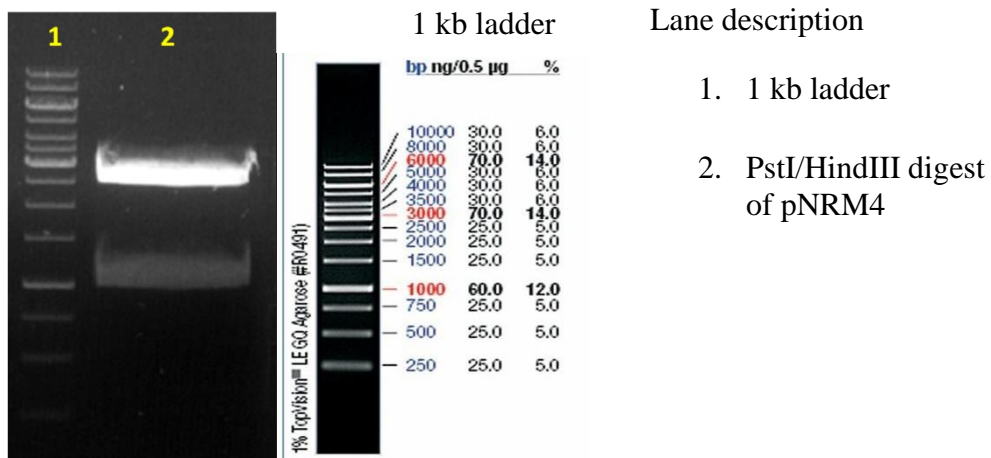


Fig. 4.6: Restriction digestion analysis of pNRM4.

4.4.1.2 Construction of pNRM5

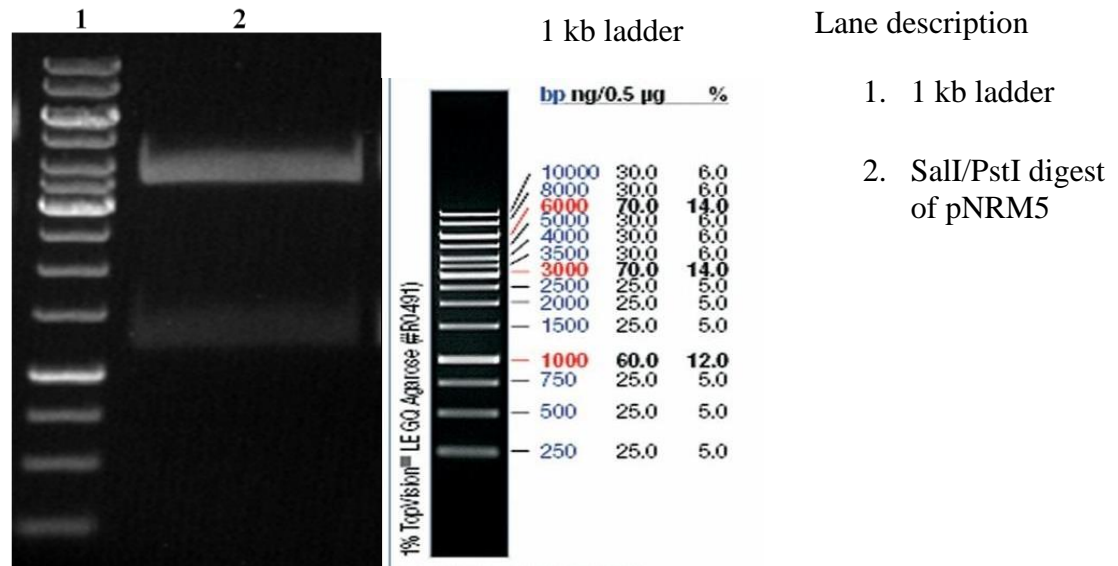


Fig. 4.7: Restriction digestion analysis of pNRM5.

4.4.1.3 Construction of pNRM6

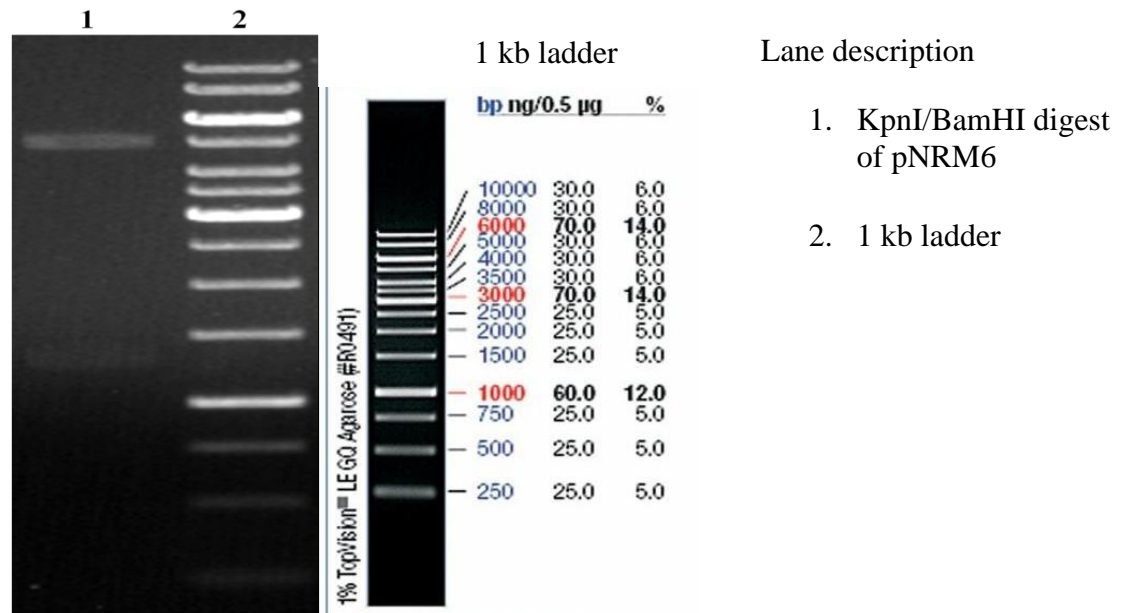


Fig. 4.8: Restriction digestion analysis of pNRM6

4.4.1.4 Construction of pNRM110

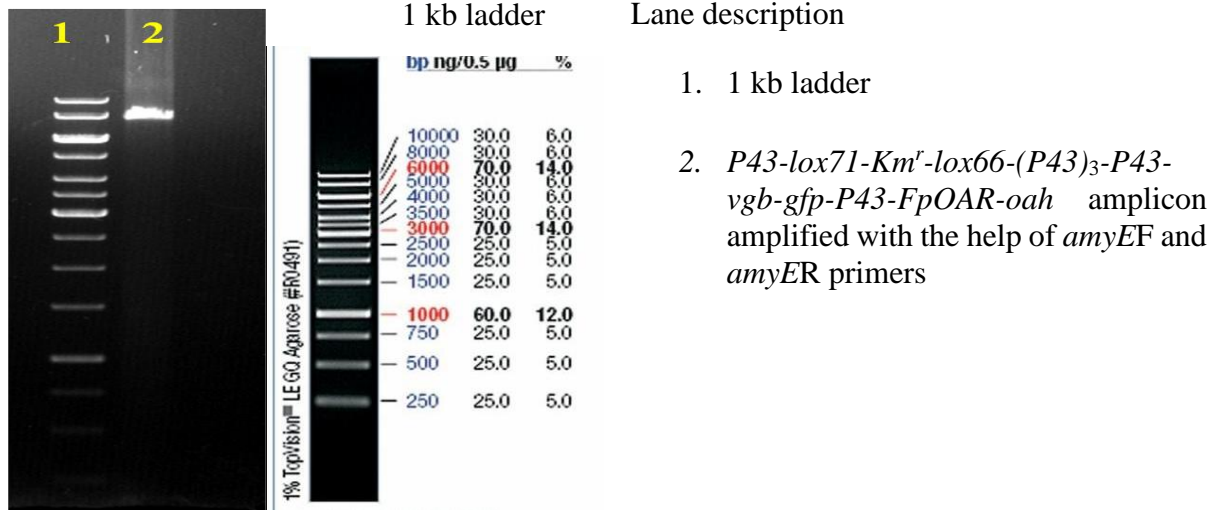


Fig. 4.9: PCR amplification of entire cassette *P43-lox71-Km^r-lox66-(P43)₃-P43-vgb-gfp-P43-FpOAR-oah* from pNRM110 using *amyEF* and *amyER*.

4.4.2 Selection of integrants DK1042 NRM110 using starch agar assay

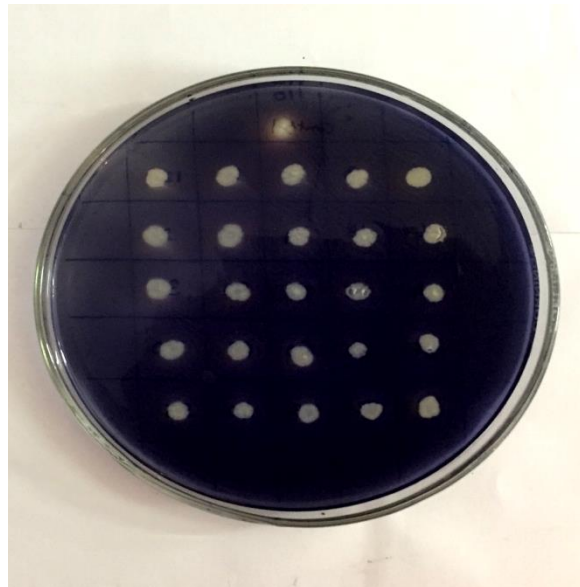


Fig. 4.10: Screening of kanamycin resistant colonies on starch agar plate

As mentioned in section 2.3.7.2, double crossover homologous recombination events were confirmed by screening kanamycin resistant DK1042 colonies on starch agar plate for the absence of amylase activity (**Fig. 4.10**). Due to successful integration

at *amyE* locus through double crossover homologous recombination, *amyE* locus in the genome of DK1042 is disrupted and absence of starch hydrolysis zone surrounding the integrant colonies facilitates the selection of correct integrants.

4.4.3 Effect of heterologous expression of artificial oxalate operon on oxalic acid secretion

4.4.3.1 Oxalic acid secretion by *E. coli* BL21DE3 pNRM5 transformant

pNRM5 is high copy number vector containing *FpOAR-oah* operon under the control of constitutive promoter *P43*. Although *P43* is originally a *B. subtilis* promoter but it is functional in *E. coli* host as well, therefore, before proceeding for the construction of integration vector the functionality of *P43-FpOAR-oah* was checked by determining the oxalic acid secretion by *E. coli* BL21DE3 harboring pNRM5 plasmid. Since *E. coli* BL21DE3 WT, *E. coli* BL21DE3 harboring pUC18 did not possess artificial oxalate operon, they were taken as controls. *E. coli* BL21DE3 WT, BL21DE3 (pUC18) and BL21DE3 (pNRM5) strains were grown in the tris rock phosphate broth (Section 2.2.3) till the pH of the medium was reduced from 8.0 to 6.0. Culture supernatants were collected and HPLC was carried out to detect the presence of oxalic acid. According to the analytical protocol and the column, oxalic acid elutes the first due to its highly polar and low molecular weight properties. Pure standard of oxalic acid was eluted at the retention time of 3.89 min and very small peaks were found in the culture supernatant of *E. coli* BL21DE3 WT and BL21DE3 vector control but a clearly distinct peak was observed in the chromatogram generated from the culture supernatant of *E. coli* BL21DE3 harboring *P43-FpOAR-oah* operon at the retention time of 3.96 min. The amount of oxalic acid secreted by *E. coli* BL21DE3 (pNRM5) was calculated in comparison to oxalic acid standard by subtracting the peak area of *E. coli* BL21DE3 WT and it was found that 2.22 mM oxalic acid was secreted in the culture medium containing 100 mM Glucose and 50 mM Tris (pH 8.0) by *E. coli* BL21DE3 (pNRM5). (Table 4.2). Figures 4.11, 4.12, 4.13, 4.14 and 4.15 show the chromatograms of standard oxalic acid (50 mM), Tris rock-phosphate broth, culture supernatant of *E. coli* BL21DE3 WT, culture supernatant of *E. coli* BL21DE3 WT

carrying pUC18 vector control and culture supernatant of *E. coli* BL21DE3 WT carrying pNRM5, respectively.

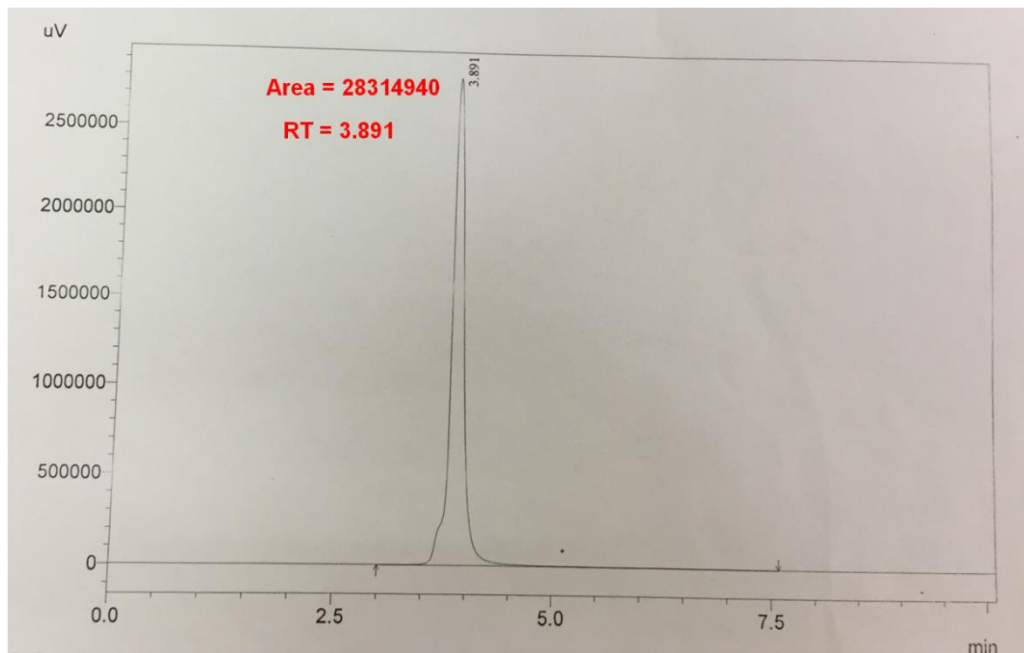


Fig. 4.11: Chromatogram of oxalic acid standard (50mM).

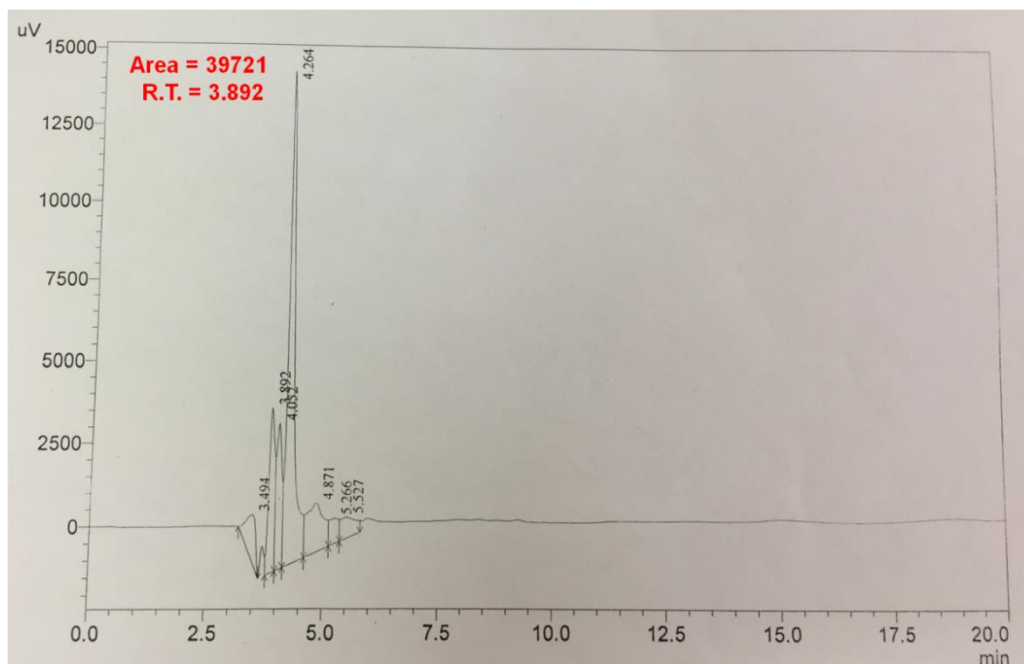


Fig. 4.12: Chromatogram of tris rock phosphate broth.

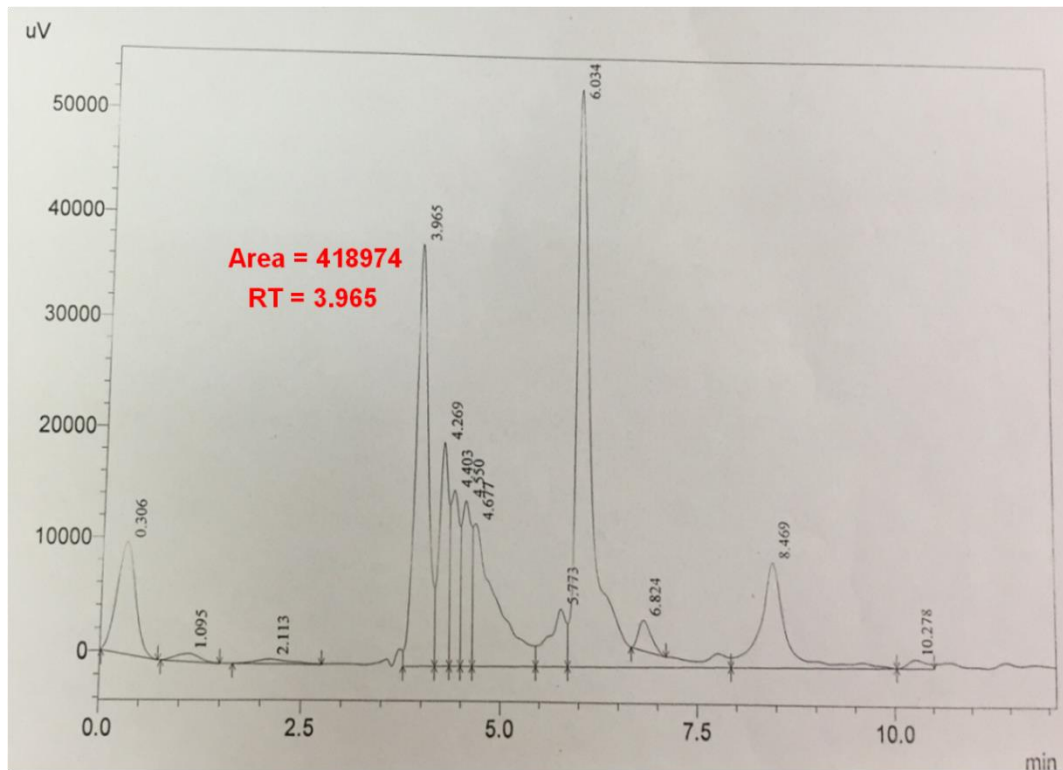


Fig. 4.13: Chromatogram of *E. coli* BL21DE3 WT culture supernatant.

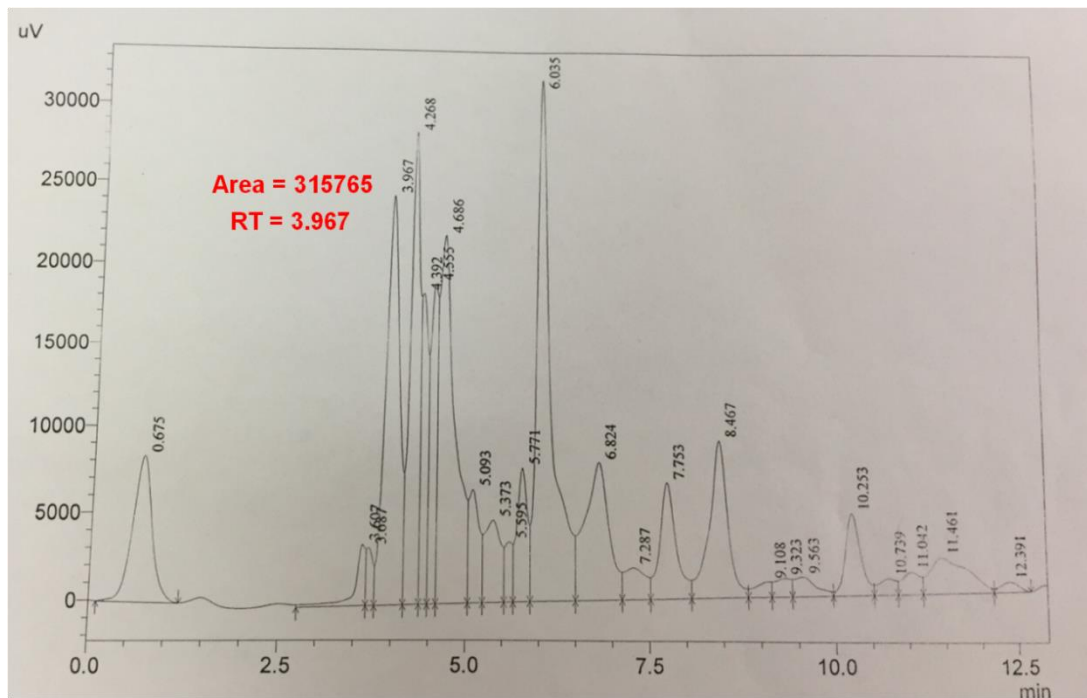


Fig. 4.14: Chromatogram of *E. coli* BL21DE3 (pUC18) (vector control) culture supernatant.

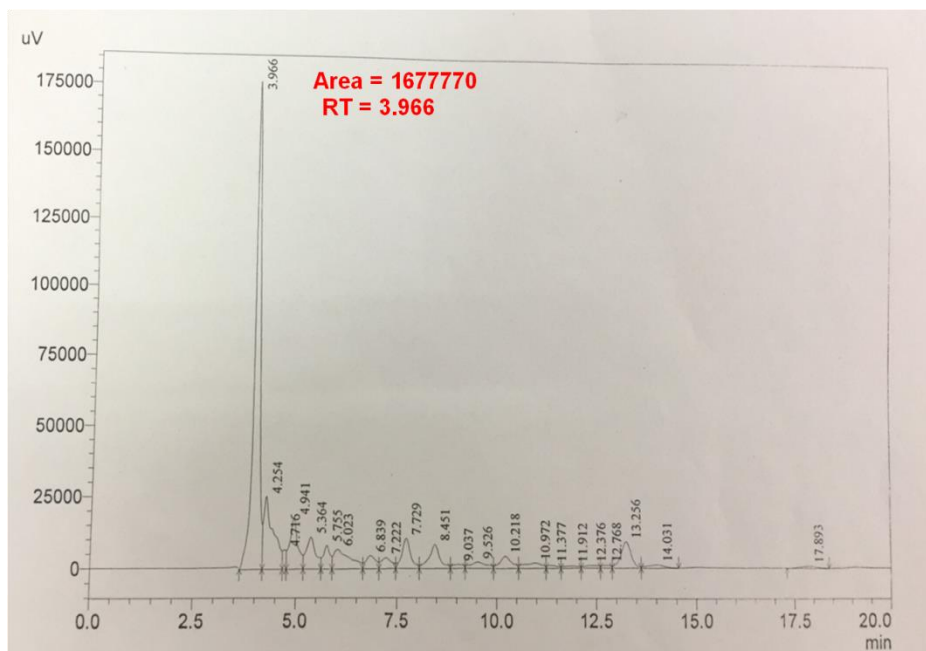
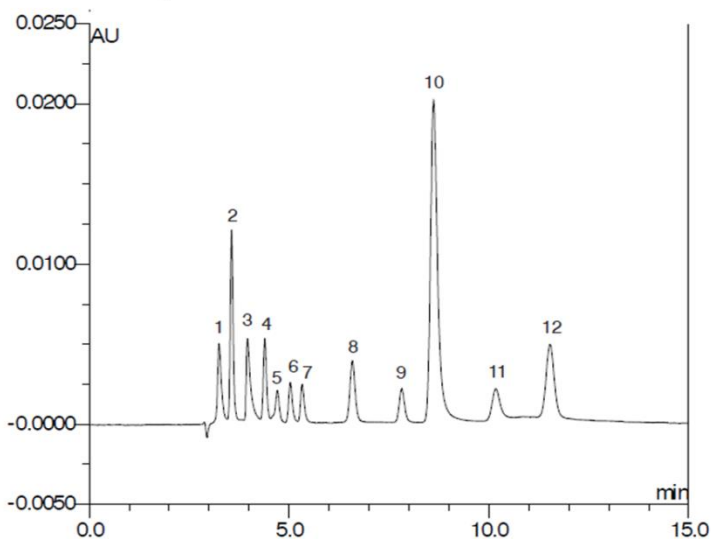


Fig. 4.15: Chromatogram of supernatant of *E. coli* BL21DE3 culture carrying pNRM5 plasmid.

Column: Acclaim OA, 5 μ m
 Dimensions: 4 x 250 mm
 Mobile Phase: 100 mM Na₂SO₄, pH 2.65 (adjusted with methanesulfonic acid)
 Temperature: 30 °C
 Flow Rate: 0.6 ml/min
 Injection Volume: 5 μ L
 Detection: UV, 210 nm



Analytes	mg/L (ppm)
1. Oxalic acid	15
2. Tartaric acid	120
3. Formic acid	180
4. Malic acid	120
5. <i>iso</i> -Citric acid	120
6. Lactic acid	180
7. Acetic acid	120
8. Citric acid	120
9. Succinic acid	120
10. Fumaric acid	7
11. <i>cis</i> -Aconitic acid	**
12. <i>trans</i> -Aconitic acid	**

** 7 ppm total for *cis* and *trans* isomers

Fig. 4.16: Example chromatogram provided in the brochure of Acclaim Organic Acid (OA) column.

Table 4.3 Comparison of oxalic acid peaks

Peak Retention Time (min)	Oxalic acid standard (50 mM) Area (mAU)	TRP Medium blank Area (mAU)	<i>E. coli</i> BL21DE3 WT Area (mAU)	<i>E. coli</i> BL21DE3 pUC18 Area (mAU)	<i>E. coli</i> BL21DE3 pNRM5 Area (mAU)
3.891 (Oxalic acid)	28314940	39721 (0.73 mM)	418974 (0.73 mM)	315765 (0.55 mM)	1677770 (2.22 mM)

4.4.3.2 Growth, pH profile and oxalic acid secretion by *B. subtilis* DK1042 NRM110

Oxalic acid production and secretion by DK1042 NRM110 was determined using HPLC of bacterial culture supernatant. As *B. subtilis* DK1042 WT, DK1042 NRM1113 and DK1042 NRM1114 do not possess oxalate operon, they were taken as control. Growth and pH of DK1042 WT and integrants was monitored in M9 minimal broth at regular time intervals to analyze acid secretion. There was no significant difference in growth pattern and pH of the integrants as compared to DK1042 WT in M9 minimal medium containing Glucose (50 mM) as a sole carbon source and combination of Glucose and Malate (50 mM + 20 mM) at 200 RPM till 48 h. (**Fig. 4.17 and 4.18**). After 24 h, the pH of the medium dropped maximum at 6.39, 6.46, 6.44 and 6.32 in DK1042 WT, DK1042 NRM1113, DK1042 NRM1114 and DK1042 NRM110 cultures grown in M9 glucose broth respectively. On the other hand, the maximum pH drop was 6.59 and 6.51 in DK1042 WT and DK1042 NRM110 cultures grown in M9 glucose + malate broth, respectively.

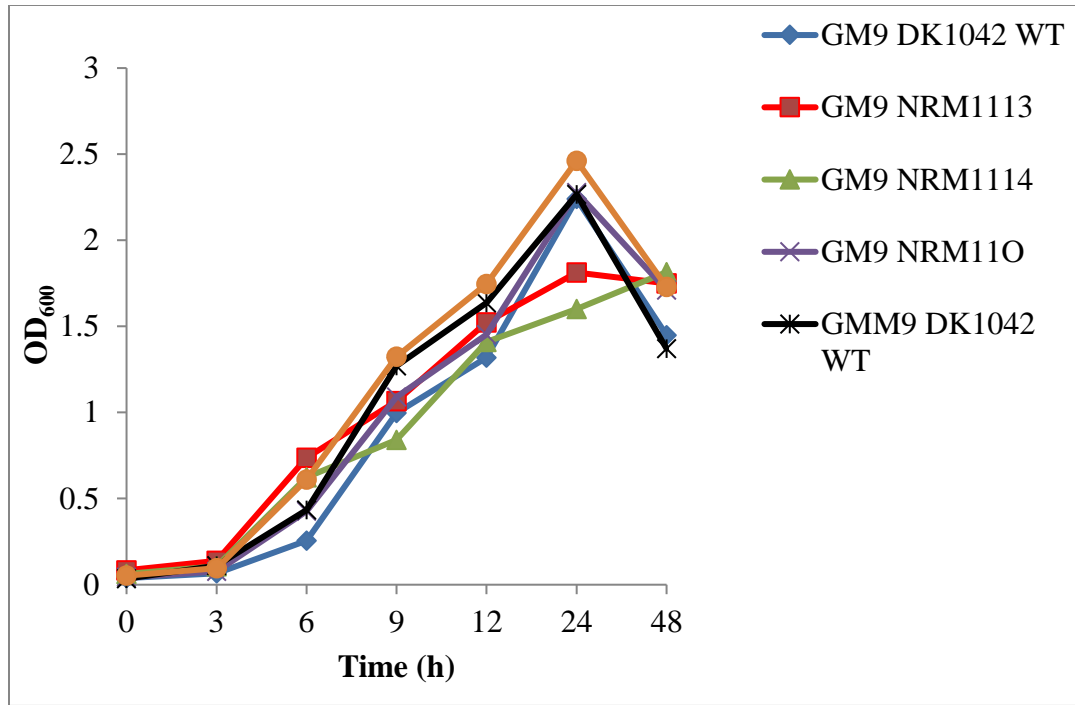


Fig. 4.17: Growth Curve of *B. subtilis* DK1042 and the integrants in M9 Minimal Medium at 200 RPM.

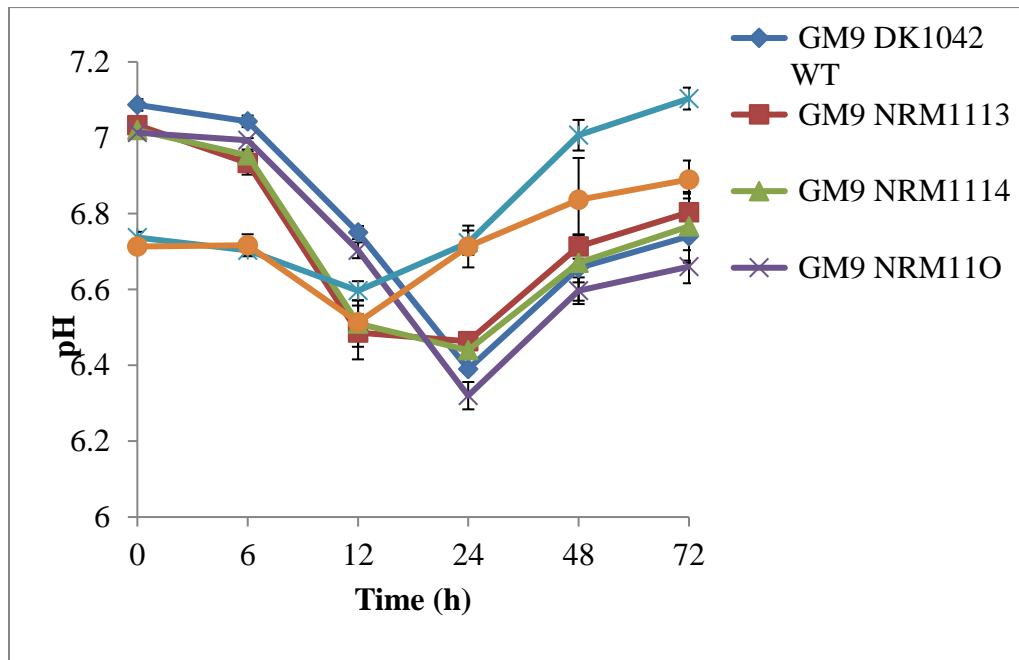


Fig. 4.18: pH profile of *B. subtilis* DK1042 and the integrants in M9 minimal medium at 200 rpm

Moreover, cells started undergoing sporulation so, after 72 h, culture supernatant from all four DK1042 WT, DK1042 NRM1113, DK1042 NRM1114 and DK1042 NRM11O cultures were taken out and HPLC was carried out to detect the presence of oxalic acid. Figures 4.19, 4.20 and 4.21 show the chromatograms of standard oxalic acid, culture supernatant of DK1042 WT and NRM11O, respectively. Oxalic acid was detected in the culture supernatant of NRM11O while it was not detected in the culture supernatant of integrants NRM1113, NRM1114 and DK1042 WT. NRM11O secreted 305 mM and 178 mM oxalic acid in M9 Glucose and M9 Glucose + Malate minimal medium, respectively.

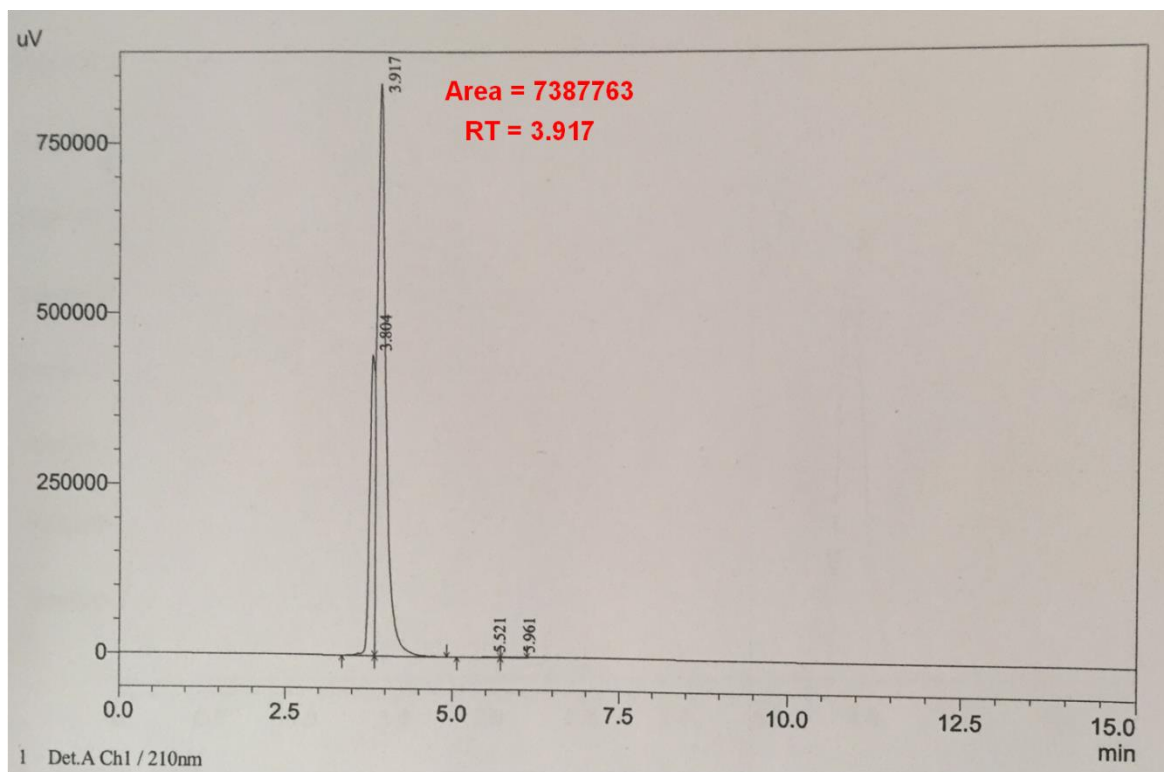


Fig. 4.19: Chromatogram of oxalic acid standard (10mM).

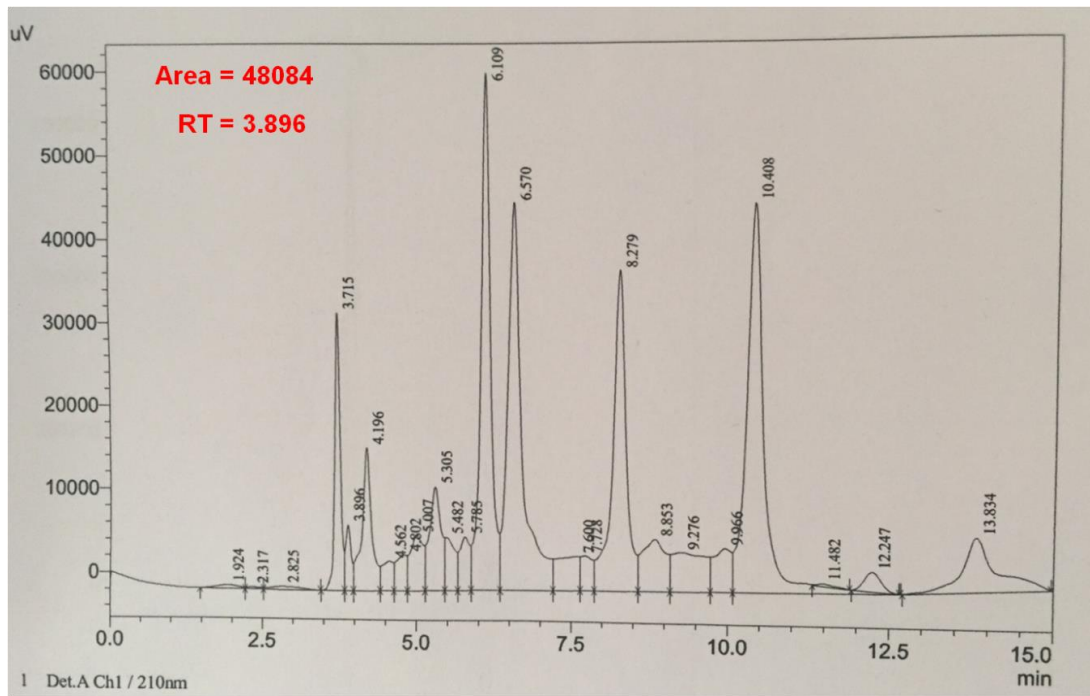


Fig. 4.20: Chromatogram of culture supernatant of *B. subtilis* DK1042 WT.

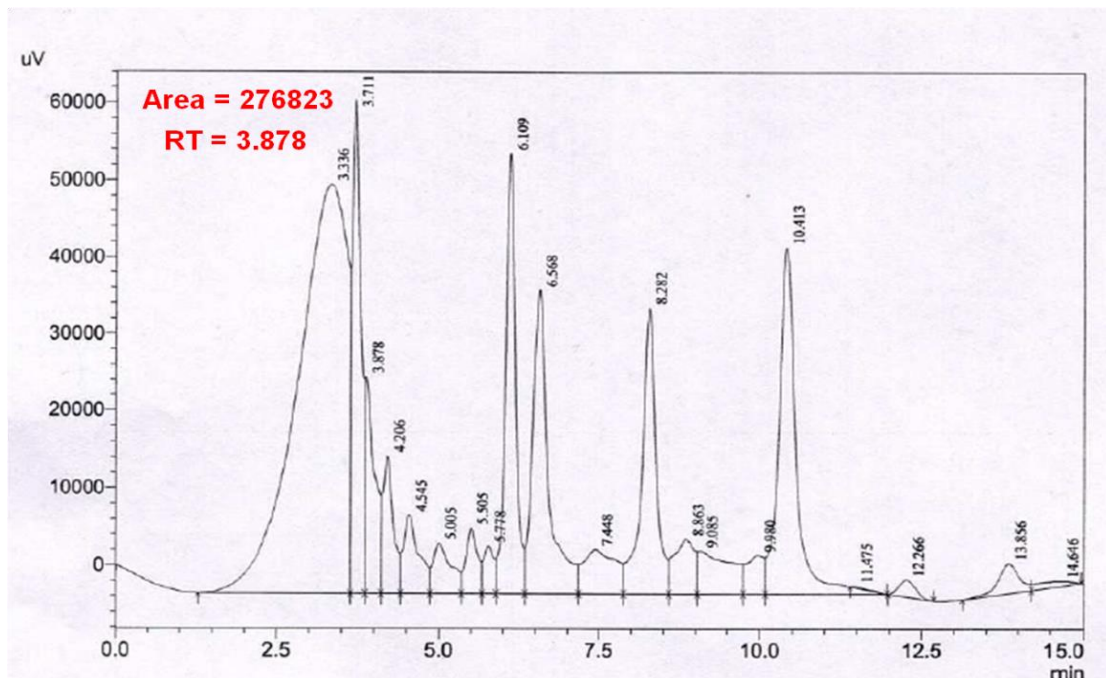


Fig. 4.21: Chromatogram of culture supernatant of *B. subtilis* DK1042 NRM1110.

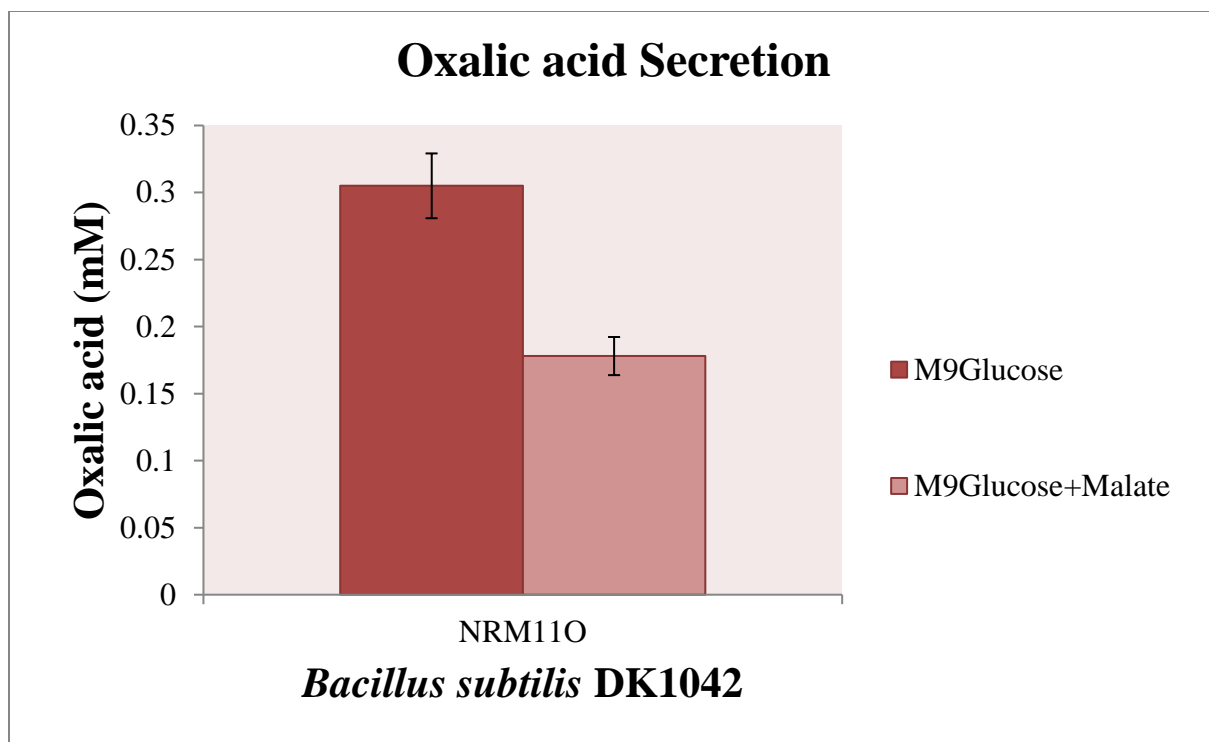


Fig. 4.22: Oxalic acid detection and Quantification by HPLC.

Glucose is the most preferred carbon source utilized by *B. subtilis* but unlike many other carboxylic acids, malate is rapidly metabolized by it (Doan et al., 2003), allowing for a similar doubling time as with glucose due to absence of catabolite repressor (*cre*) binding sites upstream of the *maeN* gene encoding the malate-Na symporter involved in the transport of Malate (Wei et al., 2000). Malate is one of the most abundant metabolites present in the root exudates of the plants (Bais et al., 2006). Oxaloacetate, the precursor for oxalic acid is synthesized from malate during TCA cycle therefore, combination of glucose and malate was used as a carbon source with an idea to increase the amount of OAA which in turn, may increase the production and secretion of oxalic acid. Contrary to our assumption, higher oxalic acid was secreted by *B. subtilis* NRM110 in presence of glucose than that produced in presence of combination of glucose and malate. Oxaloacetate occurs at the very important place of anaplerotic node and it is used to replenish the citric acid cycle and for the synthesis of several amino acids. So, it is possible that the activity of the enzymes other than OAH that use

oxaloacetate as a substrate could be higher than OAH. Our aim was to develop *B. subtilis* DK1042 genomic integrant that can secrete oxalic acid in the range of 5 – 10 mM that can be sufficient to solubilize phosphate and potassium minerals in the rhizosphere. Kleijn et al. (2010) reported that during growth on malate, malate was converted to oxaloacetate and pyruvate and much of the oxaloacetate was converted to PEP, resulting in high gluconeogenic fluxes and overflow metabolism of pyruvate and acetate and only 10% of the malate was respired via the TCA cycle, whereas the majority was secreted as overflow metabolites. Our results are in well accordance with this observation and we obtained 0.305 mM and 0.178 mM oxalic acid in M9 Glucose and M9 Glucose + Malate minimal medium, respectively.

4.4.4 Characterization of MPS and MKS ability of *B. subtilis* DK1042 and the integrants

MPS and MKS ability of *B. subtilis* DK1042 and the integrants were determined qualitatively by plate assay using Pikovaskya's agar and Aleksandrov media, respectively (Fig. 4.23). *Enterobacter asburiae* PSI3 is a Gram-negative bacterium, reported to secrete 50 mM gluconic acid (Gyaneshwar et al., 1999) and it was used as a positive control.

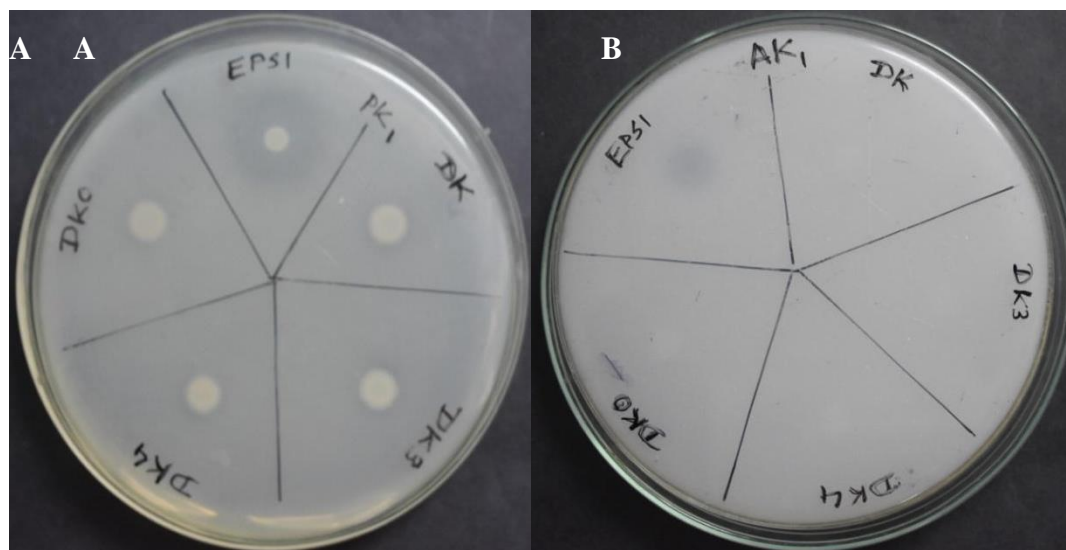


Fig. 4.23: (A) Mineral phosphate solubilization and (B) Mineral potassium solubilization by *E. asburiae* PSI3 (EPSI), *B. subtilis* DK1042 and the integrants.

It is clearly evident from the zone of clearance that *E. asburiae* PSI3 is able to solubilize both phosphorous and potassium in the respective medium due to its ability to secrete very high amounts of gluconic acid. While there is no significant difference between the diameter of the zone of clearance formed by *B. subtilis* DK1042 WT and the integrants on Pikovaskaya's agar. Neither the integrants NRM1113, NRM1114, NRM110 nor DK1042 WT formed a zone of clearance on the Aleksandrov agar. With this approach, we could incorporate oxalic acid production and secretion ability in *B. subtilis* DK1042 but the yield of oxalic acid was not sufficient enough to impart mineral phosphate and potassium solubilization ability.

4.5 Conclusion

Our broad aim was to incorporate traits which can enhance the biofertilizer potential of *B. subtilis* DK1042. With this approach, we could incorporate oxalic acid production and secretion ability in *B. subtilis* DK1042 but the yield of oxalic acid was not sufficient enough to impart mineral phosphate and potassium solubilization ability. Oxalic acid in the range of 5 – 10 mM is required to solubilize mineral complexes in the rhizosphere. As explained in the **section 3.5**, here also use of multipromoter P43 tandem repeat system could have resulted in overexpression of OAH and FpOAR proteins but Oxaloacetate – a precursor for synthesis of oxalic acid, occurs at the very important place of anaplerotic node and it is used to replenish the citric acid cycle and for the synthesis of several amino acids so, it is possible that the activity of the competitive enzymes such as Malate dehydrogenase (Mdh), phosphoenol pyruvate carboxykinase (PckA), citrate synthase (CitZ) and aspartate aminotransferase (AAT) that use oxaloacetate as a substrate could be higher than OAH because of which we could not achieve higher production and secretion of oxalic acid in *B. subtilis* DK1042.